Rare Metal Materials and Engineering
Volume 50, Issue 6, June 2021
Available online at www.rmme.ac.cn

Science Press

Cite this article as: Chen Junhong, Xu Weifang, Zhang Fangju, et al. Strain Rate Dependent Tension Behavior of TC11 Titanium Alloys[J]. Rare Metal Materials and Engineering, 2021, 50(06): 1883-1889.

ARTICLE

Strain Rate Dependent Tension Behavior of TC11 Titanium Alloys

Chen Junhong[1,2], Xu Weifang[1,2], Zhang Fangju[1,2], Zhang Jun[1,2], Chen Gang[1,2]

[1] Institute of Systems Engineering, China Academy of Engineering Physics, Mianyang 621999, China; [2] Shock and Vibration of Engineering Materials and Structures Key Laboratory of Sichuan Province, Mianyang 621999, China

Abstract: In order to investigate the effect of strain rate on the tension behavior of TC11 titanium alloy, uniaxial tensile tests were conducted on this material over a wide range of strain rate. The results demonstrate that as the strain rate increases from quasistatic to dynamic, the yield strength of the TC11 titanium alloy increases slightly. The reduction of the strain hardening modulus is found under dynamic tension. Furthermore, the TC11 titanium alloy fails in shear under both the quasistatic and dynamic tension. However, the dimple size under dynamic fracture is smaller than that under quasistatic loading. By analyzing the temperature rise in the material during deformation, it is found that the easier strain softening and the smaller dimple size on the fracture surface at high strain rate may be attributed to the higher temperature rise.

Key words: TC11 titanium alloy; strain rate; tension behavior; failure mode; temperature rise

According to the type of the microstructure, the titanium alloy can be classified as α-type, β-type and $\alpha+\beta$-type. Compared to the other two alloys, the $\alpha+\beta$-type titanium alloy has even better properties. It exhibits excellent high temperature properties, low mass, high room temperature strength, high tolerance resistance, etc. These prompt this alloy to be used in a wide variety of applications such as aircraft engine and structural components to bio-applications[1-5]. During the actual applications, the titanium alloy may be subjected to extreme environments and loading conditions such as high speed impact. Therefore, it is necessary to investigate the mechanical response of the titanium alloys under various strain rates.

The TC11 titanium alloy, which has the normal composition of Ti-Al(5.8~7.0)-Mo(2.8~3.8)-Zr(0.8~2.0)-Si(0.2~0.35), is a typical $\alpha+\beta$-type titanium alloy. During the past several years, much attention has been paid on the dynamic mechanical properties of the Ti-6Al-4V (TC4), which is the most widely used $\alpha+\beta$-type titanium alloy[6-12]. Peirs et al performed high strain rate in-plane shear and tensile tests on the Ti-6Al-4V titanium alloy[12]. Combined with the numerical approach, the stress-strain behavior of this alloy was determined. Compared to the Ti-6Al-4V, TC11 titanium alloy has a higher strength. However, restricted work has been conducted to study the dynamic mechanical properties of this titanium alloy. Tensile experiments were carried out on the Ti-6.6Al-3.3Mo-1.8Zr-0.29Si alloy at quasistatic and dynamic strain rate by Zhang and Wang[13,14]. It is found that the mechanical properties of this alloy are dependent on the strain rate. The tension yield strength increases with increasing the strain rate. However, the strain hardening behavior reduces at high strain rate. It is known that heat will be generated in the material due to the transition of plastic deformation work, which further results in temperature rise. This temperature rise, which will soften the strength of material, is related to the time scale of loading reflected by the strain rate. Then, the key problem of studying the TC11 titanium alloy is how the temperature rise couples with the strain hardening and strain rate hardening to affect the mechanical behavior. Furthermore, from the previous studies, it can be concluded that the TC4 alloy usually fractures by generating and propagating adiabatic shear band. Then, for the TC11 titanium alloy, these problems such as how the strain rate affects the fracture mode deserve further investigation.

Received date: June 10, 2020
Foundation item: National Natural Science Foundation of China (11602257, 11602256, 11572299)
Corresponding author: Chen Junhong, Ph. D., Associate Professor, Institute of Systems Engineering, China Academy of Engineering Physics, Mianyang 621999, P. R. China, Tel: 0086-816-2484403, E-mail: chenjh@lnm.imech.ac.cn

In this study, the quasistatic and dynamic tensile experiments were conducted on the TC11 titanium alloy, aiming to investigate the effect of the strain rate on the mechanical properties of this alloy. For each tested specimen, the failure mode and the fracture surface were carefully examined. Based on the experimental observation and temperature rise analysis, the strain rate dependent tension deformation behavior of the TC11 titanium alloy was discussed. The localized deformation temperature as a function of distance and time was obtained as well. Our present results may increase the understanding of the deformation and fracture mechanism of TC11 titanium alloy.

1 Experiment

The chemical composition of the tested TC11 titanium alloy was Ti-6.6Al-3.3Mo-1.8Zr-0.29Si. The specimen used in the present study was obtained from the commercial forged rods without any heat treatment process. The microstructure of this alloy is shown in Fig.1.

Quasistatic tensile tests were conducted by the material test machine, with the sample gauge section dimensions of 5 mm in diameter and 25 mm in length. The average strain rates, controlled by the velocity of the load head, were about 1×10^{-3} and 1×10^{-2} s^{-1}. Dynamic tensile tests were performed by the split Hopkinson tension bar (SHTB) apparatus. The schematic illustration of this apparatus is shown in Fig.2. During the test, the hammer impacts the block at a high speed, which induces the deformation and even fracture of the prefixed metal bar. This further generates the tensile pulse in the incident bar. The amplitude and duration of incident pulse can be controlled by adjusting the length and diameter of the prefixed metal bar and the impact velocity of the hammer. The tensile incident pulse propagates towards the specimen. When encountering the specimen, one part of the incident pulse reflects back to the incident bar, and at the same time, the other part transmits into the transmitted bar. Based on the one dimensional elastic wave propagation theory and the assumption of stress equilibrium in the specimen, the tension stress, tension strain rate and tension strain can be calculated according to the incident wave $\varepsilon_I(t)$, measured by the gauges on the incident bar, and the transmitter wave $\varepsilon_T(t)$, measured by the gauges on the transmitted bar as follows:

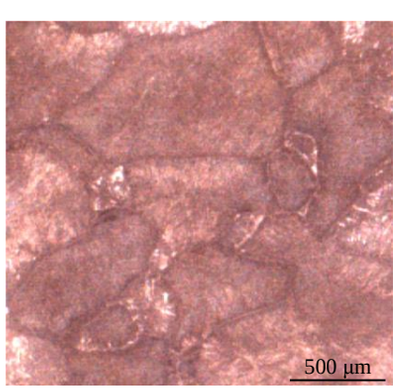

Fig.1 Microstructure of the TC11 titanium alloy

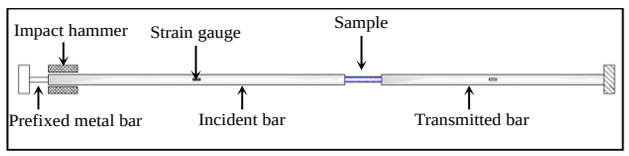

Fig.2 Schematic diagram of the split Hopkinson tension bar

$$\sigma = \frac{A_0}{A_s} E\varepsilon_T(t) \quad (1)$$

$$\dot{\varepsilon}(t) = \frac{2C_0}{L} [\varepsilon_I(t) - \varepsilon_T(t)] \quad (2)$$

$$\varepsilon(t) = \frac{2C_0}{L} \int_0^t [\varepsilon_I(t) - \varepsilon_T(t)] \mathrm{d}t \quad (3)$$

where C_0, E and A_s are elastic wave velocity, elastic modulus and cross section area of the bar, respectively; A_0 and L are initial cross section area and length of the specimen gauge section, respectively. In the present test, the prefixed metal bar with 8 mm in diameter was used to keep the average strain rate of 3.2×10^2 s^{-1}, while 10 mm was used to keep the strain rate of 1.2×10^3 s^{-1}. To obtain reliable test results at different strain rates, at least four specimens were performed for each case. After testing, the failure modes and the fracture surfaces of all specimens were carefully checked.

2 Results

2.1 Stress-strain behavior

Fig. 3 shows the true stress-strain curves of the TC11 titanium alloy under quasistatic and dynamic tension. The specimens at the strain rate of 3.2×10^2 s^{-1} only experience plastic deformation. From this figure, it can be seen that the TC11 titanium alloys have different strength and ductility values at one strain rate. This dispersion of strength and ductility may be attributed to the fact that the mechanical properties of this alloy are sensitive to the flaws which come from material preparation or specimen machining. Fig. 4 shows the typical true stress-strain curves of the TC11 titanium alloy under quasistatic and dynamic strain rate. It can be seen that the deformation process can be divided into three stages. Upon loading, the material responds elastically first. Just after yielding, the material demonstrates approximately linear stress-strain relation because the differential of the stress-strain curve shown in Fig. 5 maintains a constant value. After that, nonlinear decrease of the stress occurs, followed by the rapid drop of stress, indicating the fracture of the specimen.

The variation of yield strength with strain rate is shown in Fig. 6. As the strain rate increases from 1.0×10^{-3} s^{-1} to 1.2×10^3 s^{-1}, the average yield strength changes slightly from 1.03 GPa to 1.23 GPa. It can be seen from Fig. 4 that the TC11 titanium alloy exhibits different strain hardening abilities under various strain rates. In order to quantitatively characterize the strain hardening behavior, linear fitting is conducted on the second

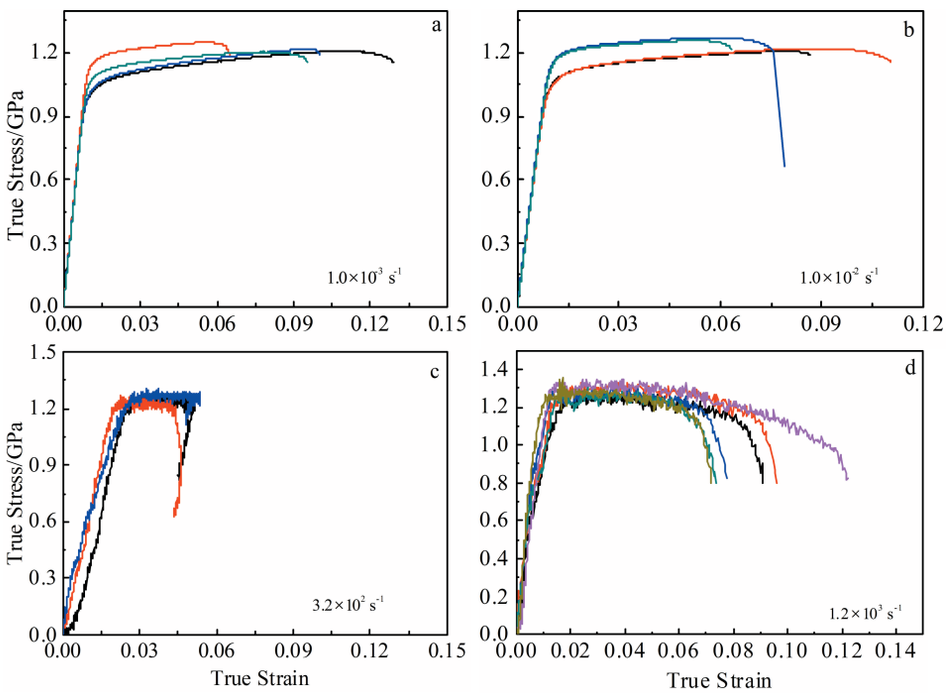

Fig.3 True tensile stress-strain curves of the TC11 titanium alloy under different strain rates: (a) 1.0×10^{-3} s^{-1}, (b) 1.0×10^{-2} s^{-1}, (c) 3.2×10^{2} s^{-1}, and (d) 1.2×10^{3} s^{-1}

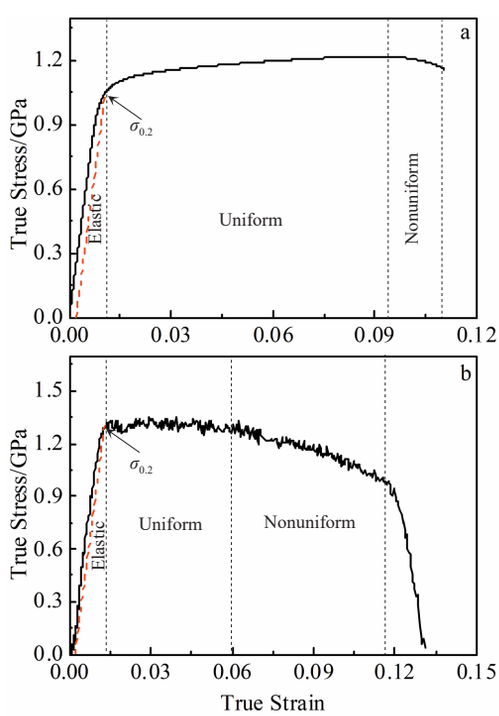

Fig.4 True stress-strain curves under different strain rates: (a) 1×10^{-3} s^{-1} and (b) 1.2×10^{3} s^{-1}

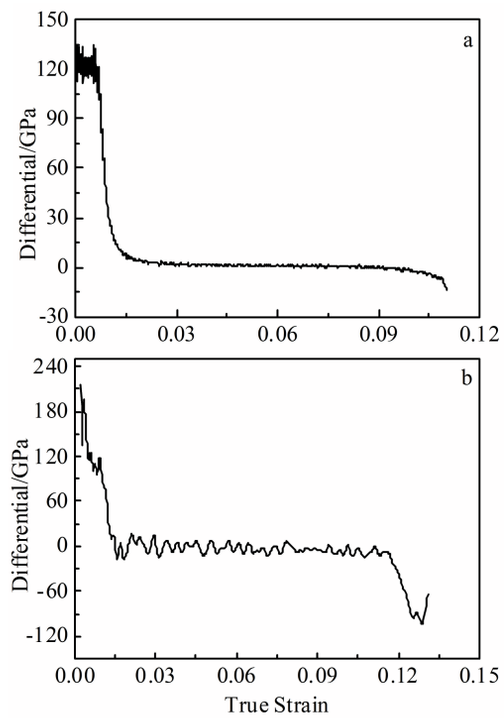

Fig.5 Differential of the stress-strain curve of the TC11 titanium alloy under different strain rates: (a) 1×10^{-3} s^{-1} and (b) 1.2×10^{3} s^{-1}

deformation stage of the TC11 titanium alloy. The slope of the fitting curve is taken as the linear strain hardening modulus. The variation of linear strain hardening modulus with strain rate is shown in Fig. 7. From this figure, it can be seen that with increasing the strain rate, the linear strain hardening modulus decreases from 1.5 GPa to -0.8 GPa. This indicates that strain hardening disappears under high strain rate. Strain softening dominates the deformation of the TC11 titanium

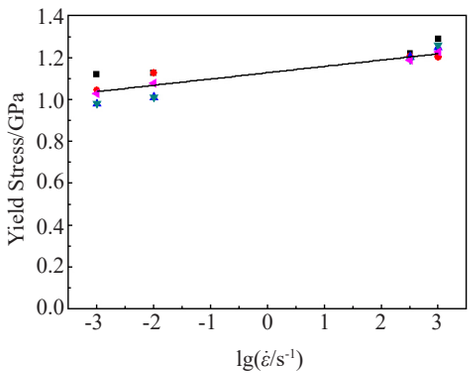

Fig.6 Variation of yield strength of TC11 titanium alloy with strain rate

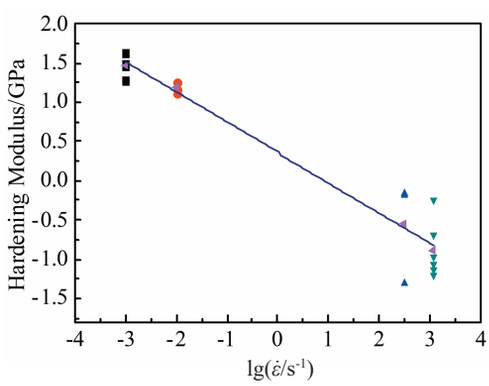

Fig.7 Variation of linear strain hardening modulus of TC11 titanium alloy with strain rate

alloy under dynamic loading.

2.2 Fracture morphologies

Fig. 8 shows the macroscopic deformation and fracture morphologies of TC11 titanium alloy at the strain rate of 1.0×10^{-3} s^{-1}. It can be seen from Fig. 8a that the specimens fail by shearing. The magnification of the area marked in Fig. 8a is shown in Fig. 8b. The specimen has a rough shear fracture surface. This is different from the brittle material such as metallic glass which has a smooth tensile fracture surface[15,16]. Furthermore, the specimen does not exhibit visible necking near the fracture surface. Typical cell-like and river-like vein patterns are observed on the fracture surface, as shown in Fig. 8c and 8d, respectively. The cell-like vein pattern is the typical fracture morphology of titanium alloy under dynamic shear loading, while the river-like vein pattern is the typical tensile fracture morphology[17-21]. These indicate that both the local shear and tensile fracture occur in the TC11 titanium alloy.

Fig. 9 gives the macroscopic deformation and fracture morphologies of the TC11 titanium alloy at the strain rate of 1.0×10^{-2} s^{-1}. Fig. 9b is a magnified image corresponding to the marked area in Fig.9a. As can be seen from Fig.9a and Fig.9b,

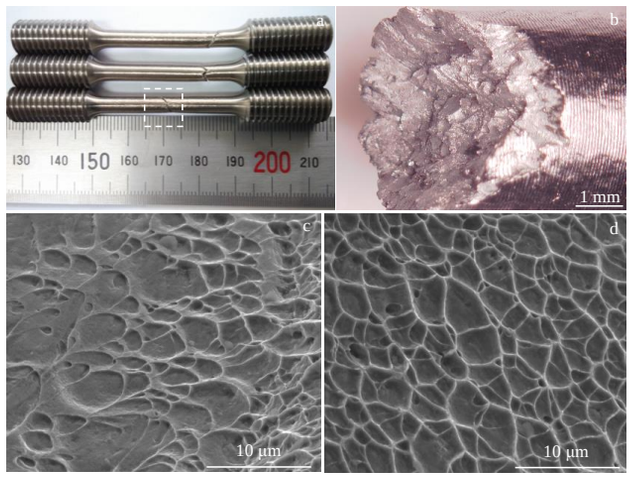

Fig.8 Fracture morphologies of TC11 titanium alloy under the strain rate of 1.0×10^{-3} s^{-1}: (a, b) specimens after fracture, (c) cell-like vein pattern, and (d) river-like vein pattern

this titanium alloy mainly fails by shearing, which is similar to the situation of 1.0×10^{-3} s^{-1} strain rate. Little necking can be observed near the fracture surface. As shown in Fig. 9c, a smooth fracture slip zone can be observed at the edge of the fracture surface, which indicates the occurrence of shear fracture in this area. This zone has the maximum width of about 70 μm. Fig. 9d and Fig. 9e show the typical morphologies in the middle of the fracture surface. Dimple-like vein pattern can be observed, indicating the tensile fracture.

Since the specimen under the strain rate of 3.2×10^{2} s^{-1} does not fail finally, the fractured specimens under the strain rate of 1.2×10^{3} s^{-1} are carefully examined, as shown in Fig. 10. Fig. 10b shows the magnification of the marked area in Fig. 10a. It can be seen that the specimen fails by shearing. Furthermore, necking can be clearly observed. This indicates that obvious nonuniform deformation occurs before fracture, which is consistent with the results mentioned in Section 2.1. Similar to the specimen under the strain rate of 1.0×10^{-2} s^{-1}, the smooth shear slip zone exists at the edge of the fracture surface. However, under dynamic loading, the width of this slip zone is 90 μm, which is larger than that of the quasistatic specimen. As shown in Fig. 10d and 10e, typical dimple-like pattern can be observed in the middle of the fracture surface, indicating the occurrence of tensile fracture. The characteristic dimple size is smaller than that in the quasistatic tension, which is consistent with the observation found by Zhang and Wang[13,14].

3 Discussion

The experimental results and observation reveal some crucial features of TC11 titanium alloy behavior during deformation, as follows. (1) Under quasistatic loading, the TC11 titanium alloy exhibits linear strain hardening behavior after yielding. However, instead of strain hardening, strain softening occurs for this alloy under high strain rate loading. (2) Uniform deformation dominates the TC11 titanium alloy

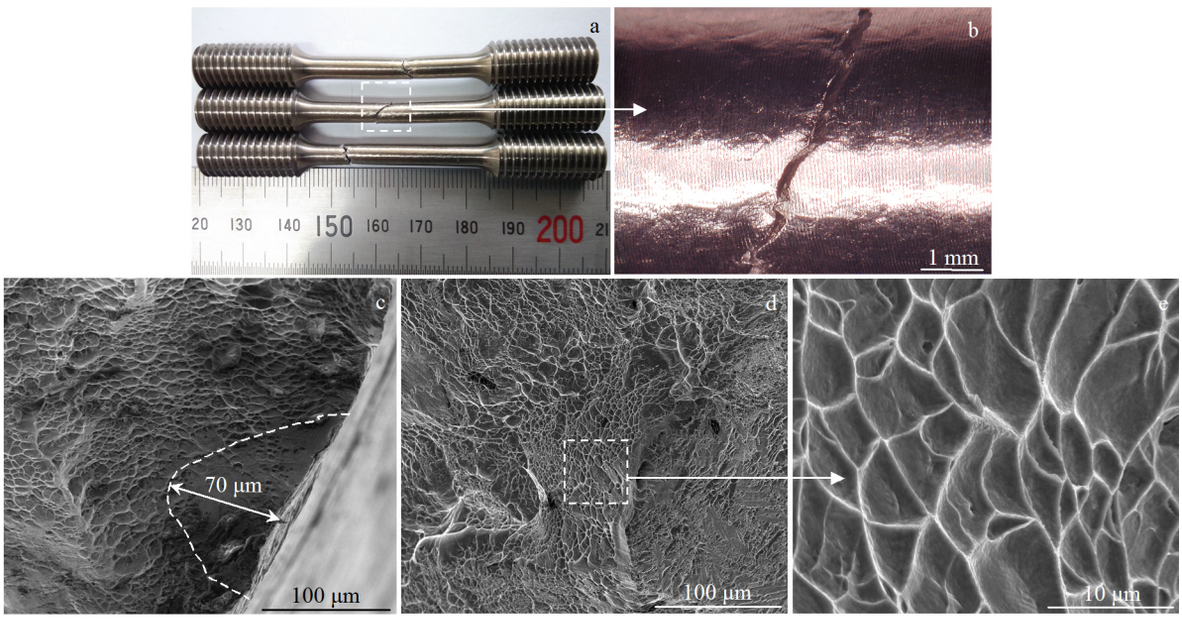

Fig.9 Fracture morphologies of the TC11 titanium alloy under the strain rate of 1.0×10^{-2} s^{-1}: (a, b) specimen after fracture, (c) edge morphology of the fracture surface, and (d, e) typical pattern in the middle of the fracture surface

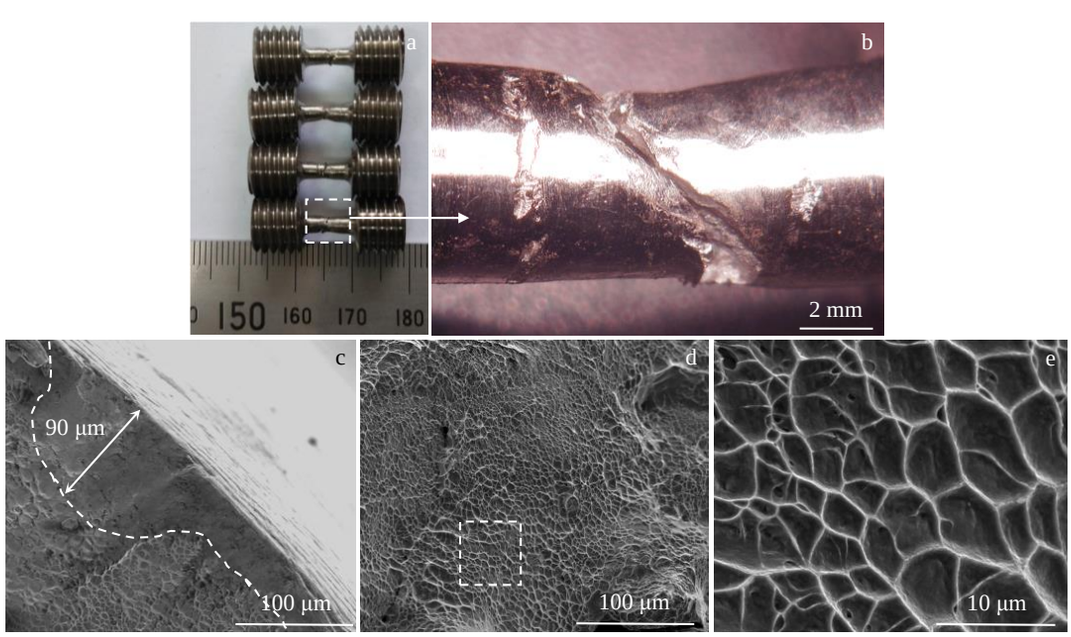

Fig.10 Fracture morphologies of the TC11 titanium alloy under the strain rate of 1.2×10^{3} s^{-1}: (a, b) fractured specimens, (c) edge morphology of the fracture surface, and (d, e) typical pattern in the middle of the fracture surface

under quasistatic loading. However, nonuniform deformation mainly occurs at high strain rate. (3) Macroscopically, the TC11 titanium alloy fails by shearing under both quasistatic and dynamic loading. Microscopically, both the local shear and tensile fracture exist on the fracture surface. Furthermore, under dynamic loading, TC11 titanium alloy has larger shear slip zone and smaller dimple size.

As aforementioned, heat will be generated in the material due to the transition of plastic deformation work, which results in temperature rise. This temperature rise will induce strength softening of material. Thus, the mechanical properties of material are affected by the competition between thermal

softening and strain hardening. The temperature rise is dependent on the plastic deformation and the thermal diffusion, as can be expressed by the following equation:

$$\frac{\partial T}{\partial t}=\kappa\frac{\sigma\dot{\varepsilon}}{\rho_{\mathrm{p}}C_{\mathrm{p}}}+\alpha\frac{\partial^2 T}{\partial^2 x} \tag{4}$$

where ρ_{p}, C_{p} are the density and specific heat of the material, respectively; $\alpha=\lambda/\rho_{\mathrm{p}}C_{\mathrm{p}}$, which is the thermal diffusion coefficient, and λ is the heat conduction coefficient; κ is the conversion factor of plastic work to heat; σ and $\dot{\varepsilon}$ are the stress and strain rate of the material, respectively; T is the temperature, t is the time, and x is the distance from the heat source. In Eq.(4), the first term in the right of the equal sign refers to the generation of the temperature, while the second term indicates the diffusion of the temperature. The temperature rise in the material is dependent on the competition between the generation of the heat and the diffusion of the temperature.

The deformation of the TC11 titanium alloy can be divided into three major processes before final failure, as shown in Fig. 4. In the first stage, no temperature is generated because the material behaves elastically. In the second deformation stage, the material demonstrates approximately linear stress-strain relation, which refers to uniform deformation. In this stage, every part of material has the same plastic deformation, indicating that the temperature is distributed uniformly in the material, no heat diffusion occurs in the material. In Eq. (4), the second term on the right of the equal sign can be ignored. However, heat will be conducted into the environment since it has lower temperature. In the quasistatic tension, the deformation process has a longer duration. The generated heat has enough time to diffuse into the environment. Thus, the uniform deformation stage acts like an isothermal process. The deformation of the TC11 titanium alloy is controlled by the strain hardening. However, under high strain rate tension, the deformation lasts for a much shorter time. The heat generated in the material does not have enough time to diffuse into the environment. This dynamic deformation stage acts like an adiabatic process. The strength softening caused by the temperature rise will control the deformation of the TC11 titanium alloy, which is why the strain hardening modulus becomes a negative value under dynamic tension.

In the third deformation stage, the stress decreases nonlinearly with increasing the strain, as shown in Fig. 4. In this stage, nonuniform deformation such as necking and local shearing occurs in the materials. The localized plastic deformation zone in the material has the highest temperature rise. From the experimental observation, the TC11 titanium alloy fails by shearing under both quasistatic and dynamic loading. According to the previous studies, if the localized shear can be treated as the planar sources of heat, the thin-film solution of Eq. (4) can be obtained. The temperature rise can be given by the following equation[22,23]:

$$T=\left(\frac{H}{2\rho_{\mathrm{p}}c_{\mathrm{p}}\sqrt{\pi\alpha}}\right)\frac{1}{\sqrt{t}}\exp\left(\frac{-x^2}{4\alpha t}\right) \tag{5}$$

where H is the heat content (energy per unit area) generated by shear. It can be given by $H=\kappa\tau_{\mathrm{y}}\psi_{\mathrm{c}}$, in which ψ_{c} is the critical shear displacement that can be measured by the value of smooth shear slip zone observed on the fracture surface, τ_{y} is the shear strength. Taking the values of parameters of the TC11 titanium alloy as follows: ρ_{p} of 4480 kg/m^3, c_{p} of 605 J/kg·K, α of 2.32×10^{-6} m^2/s. κ is the Taylor-Quinney coefficient which has the value of 0.9. From the dynamic experiments, ψ_{c} has the value of 90 μm, τ_{y} has the value of about 0.6 GPa which corresponds to the shear stress in the fracture surface. Substituting these parameters into Eq. (5), the variation of the temperature rise with the distance x can be obtained, as shown in Fig. 11. Here, five different values of time are considered.

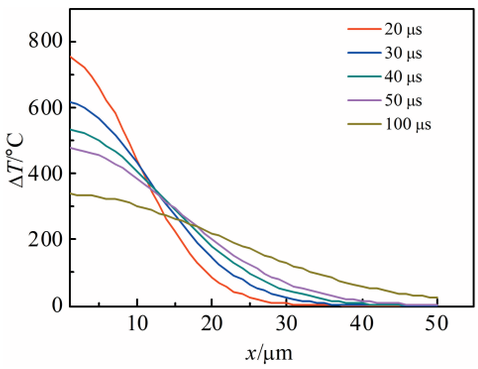

Fig.11 Variation of temperature rise with the distance to the shear fracture surface at different time

According to the experimental study of TC4 titanium alloy by Liao and Duffy [24], the temperature inside the shear band will increase from the room temperature to the maximum value during the local shear deformation. This process lasts for only 20 μs under the strain rate of 1.4×10^3 s^{-1}. Considering that the TC11 titanium alloy in this study experiences the similar strain rate with the experiment conducted by Liao and Duffy[24], the typical time of 20 μs is chosen. From Fig. 11, it can be seen that the maximum temperature rise in the shear fracture surface is 750 °C. Furthermore, the temperature rise in the shear fracture surface decreases with increasing the time. Compared to the dynamic tension, the material has smaller heat content under quasistatic situation since it has smaller shear slip zone. The duration of temperature rise under quasistatic tension should be larger than under dynamic situation due to the fact that the material has slower deformation rate. Thus, the temperature rise in the shear fracture surface under dynamic tension should be higher than under the quasistatic tension. From the previous study[25], it is found that the dimple like vein pattern in the fracture surface is related to the evolution of the micro-hole in the alloy. This evolution process is affected by the strain rate and temperature. Under dynamic tension, the higher deformation rate and temperature rise may result in smaller dimple size.

4 Conclusions

1) With increasing the strain rate, the yield strength

increases slightly from 1.03 GPa to 1.23 GPa, while the strain hardening modulus decreases from 1.5 GPa to -0.8 GPa.

2) Macroscopically, the TC11 titanium alloy fails by shearing under both quasistatic and dynamic strain rate. Microscopically, both the local shear and tensile fracture exist on the fracture surface. The dimple size becomes smaller under dynamic loading.

3) The temperature rise during nonuniform deformation stage is estimated. The maximum temperature rise can achieve 750 ℃ under dynamic tension. It is proposed that higher adiabatic temperature rise will cause the strain softening under dynamic tension, which further induces the smaller dimple size in the fracture surface.

References

1 Gorynini I V. *Materials Science and Engineering A*[J], 1999, 263: 112

2 Peters M, Kumpfert J, Ward C H *et al*. *Advanced Engineering Materials*[J], 2003, 5: 419

3 Gurrappa I. *Materials Characterization*[J], 2003, 51: 131

4 Leyens C, Peters M. *Titanium and Titanium Alloys*[M]. Weinheim: Wiley-VCH, 2003: 292

5 Rack H J, Qazi J I. *Materials Science and Engineering C*[J], 2006, 26: 1269

6 Da Silva M G, Ramesh K T. *Materials Science and Engineering A* [J], 1997, 232: 11

7 Macdougall D A S, Harding J. *Journal of the Mechanics and Physics of Solids*[J], 1999, 47: 1157

8 Nemat-Nasser S, Guo W G, Nesterenko V F *et al*. *Mechanics of Materials*[J], 2001, 33: 425

9 Khan Akhtar S, Suh Yeong Sung, Rehan Kazmi. *International Journal of Plasticity*[J], 2004, 20: 2233

10 Yuan B G, Yu H P, Li C F. *Transactions of Nonferrous Metals Society of China*[J], 2012, 22: 2943

11 Tao Z J, Fan X G, Yang H *et al*. *Transactions of Nonferrous Metals Society of China*[J], 2018, 28: 298

12 Peirs J, Verleysen P, Degrieck J. *Experimental Mechanics*[J], 2012, 52: 729

13 Zhang J, Wang Y. *Materials Letters*[J], 2014, 124: 113

14 Zhang J, Wang Y. *Materials Science and Engineering A*[J], 2014, 605: 59

15 Jiang M Q, Ling Z, Meng J X *et al*. *Philosophical Magazine*[J], 2008, 88: 407

16 Dai L H, Bai Y L. *International Journal of Impact Engineering*[J], 2008, 35: 704

17 Zhang J, Tan C W, Ren Y *et al*. *Transactions of Nonferrous Metals Society of China*[J], 2001, 21: 2396

18 Lee W S, Lin C F, Huang S Z. *Journal of Mechanical Engineering Science*[J], 2006, 220: 127

19 Guo Y Z, Li Y L. *Acta Mechanica Solida Sinica*[J], 2012, 25: 299

20 Longere P, Dragon A. *Mechanics of Materials*[J], 2015, 80: 203

21 Zhang J, Tan C W, Ren Y *et al*. *Transactions of Nonferrous Metals Society of China*[J], 2011, 21: 39

22 Lewandowski J J, Greer A I. *Nature Materials*[J], 2006, 5: 15

23 Wang J G, Pan Y, Song S X *et al*. *Materials Science and Engineering A*[J] , 2016, 651: 321

24 Liao S C, Duffy J. *Journal of the Mechanics and Physics of Solids* [J], 1998, 11: 2201

25 Hull D. *Fractography: Observing, Measuring and Interpreting Fracture Surface Topography*[M]. London: Cambridge University Press, 1999: 242

TC11钛合金应变率相关的拉伸行为

陈军红[1,2]，徐伟芳[1,2]，张方举[1,2]，张　军[1,2]，陈　刚[1,2]

(1. 中国工程物理研究院总体工程研究所，四川 绵阳 621999)

(2. 工程材料与结构冲击振动四川省重点实验室，四川 绵阳 621999)

摘　要：为了获取TC11钛合金拉伸性能随应变率的变化规律，对该材料开展了宽应变率范围下的单轴拉伸试验。结果表明，随着应变率从准静态增加到动态，TC11钛合金的屈服强度略有上升，而应变硬化模量下降。此外，在准静态和动态拉伸下，TC11钛合金均发生了剪切断裂，但动态断裂面上韧窝尺寸小于准静态断面上韧窝尺寸。进一步对材料在变形过程中的温升进行了分析，结果发现，高应变率下材料断裂面上更小尺寸的韧窝和材料更容易发生应变软化归因于动态加载情况下材料中产生了更高的温升。

关键词：TC11钛合金；应变率；拉伸行为；失效模式；温升

作者简介：陈军红，男，1987年生，博士，副研究员，中国工程物理研究院总体工程研究所，四川 绵阳 621999，电话：0816-2484403，E-mail：chenjh@lnm.imech.ac.cn